HRC TR 288

AN EG&G COMPANY

AD711963

FINAL REPORT
Contract FA70WAI-185
(Contract N00014-70-C-0374)

PENETRATION OF SONIC BOOM ENERGY INTO THE OCEAN: AN EXPERIMENTAL SIMULATION

JUNE 1970

Prepared For

DEPARTMENT OF TRANSPORTATION
FEDERAL AVIATION ADMINISTRATION
OFFICE OF NOISE ABATEMENT

HYDROSPACE RESEARCH CORPORATION
5541 NICHOLSON LANE ROCKVILLE, MARYLAND 20852

FINAL REPORT

HRC Technical Report Number 288

PENETRATION OF SONIC BOOM ENERGY INTO THE OCEAN: AN EXPERIMENTAL SIMULATION

June 1970

Prepared by
John F. Waters
Ray E. Glass

This report has been prepared for unlimited availability.

This report has been prepared by Hydrospace Research Corporation, for the Office of Noise Abatement, Federal Aviation Administration, under Contract Number FA70WAI-185 (N00014-70-C-0374). The contents of this report reflect the views of the contractor, who is responsible for the facts and the accuracy of the data presented herein, and do not necessarily reflect the official views or policy of the FAA. This report does not constitute a standard, specification or regulation.

HYDROSPACE RESEARCH CORPORATION
5541 Nicholson Lane
Rockville, Maryland 20852

SUMMARY

Penetration of sound into a body of water from a simulated airborne sonic boom was measured in an acoustically scaled experiment. Dynamite caps were used to produce spherically spreading N-waves which impinged upon the water. Microphones at the water surface and hydrophones at various shallow depths were used to measure the exponentially attenuating penetration of the airborne pressure field into the water, under total reflection conditions.

Agreement between the scaled experimental measurements and predictions based on existing theory was generally good. Application of the theory to the case of actual sonic booms impinging upon the ocean, and comparisons with measurements of typical deep-ocean ambient noise, indicate that underwater sonic boom noise will be discernible only at very low frequencies and at shallow depths. Pressure fluctuation spectrum levels due to surface waves will be higher than levels due to sonic booms.

TABLE OF CONTENTS

TABLE OF CONTENTS (Contd.)

Section 1

INTRODUCTION

1.1 BACKGROUND

In anticipation of regular supersonic aircraft operations over the ocean, the penetration of sonic boom energy into the water and particularly its effects on the ocean ecology are of current interest.

To date, there have been no conclusive experimental measurements of underwater noise due to sonic booms. One full-scale measurement has been reported,[1*] but inadequate instrumentation was used, and the position of the Mach 1.1 aircraft relative to the sensors was not tracked during this experiment.

In contrast, the theory of the transmission and penetration of acoustic energy from air to water is well established.[2] Recent theoretical studies have directly addressed the problem of penetration of sonic booms into the ocean.[3,4] In these studies, it has been assumed that the aircraft flies horizontally over a flat ocean, at a constant speed which is less than the speed of sound in the water. Under these conditions, there is total reflection of the incident shock wave. Acoustic energy penetrates only slightly into the water. Sound due to the sonic boom is attenuated rapidly with frequency and with depth in the water.

There exists a clear need for experimental measurements which can be compared with theoretical predictions of the extent to which sonic booms penetrate into the ocean. To help fill this need, some measurements of the penetration of energy from a shock wave into a small body of water have been made. Air blasts of explosive charges were used to produce shock waves having N-waveforms. Microphones

*References are listed on Page R-1

and hydrophones at various locations were used to measure the penetration of acoustic energy into the water.

The measurements obtained in this experimental simulation of the penetration of sonic boom energy into the ocean have been found to agree well with the theoretical predictions. This provides confirmation of the theoretical prediction[3] that audible noise due to sonic booms will not be appreciable at depths greater than about 15 feet in the ocean. This conclusion is, however, limited to the case of horizontal flight, constant speed less than Mach 4.5, and a flat ocean surface.

1.2 ORGANIZATION OF REPORT

In Section 2, existing theoretical predictions of the penetration of sonic boom into the ocean are summarized, and the limitations of available theory are indicated. Section 3 describes the experiment which was conducted, and Section 4 summarizes the experimental results, comparing them with the theoretical predictions. In Section 5, the anticipated penetration of sonic boom energy into the ocean at several depths is related to deep ocean ambient noise levels. Finally, the conclusions developed on the basis of this work are summarized in Section 6.

Section 2
SUMMARY OF THEORETICAL PREDICTIONS

2.1 INTRODUCTION

For a supersonic aircraft in level flight over a smooth ocean, the intersection of the Mach cone with the ocean surface is a hyperbola. The shock wavefront sweeps across the ocean surface at the speed of the aircraft.

The thickness of the sonic boom N-wave is much less than the radius of the Mach cone at its hyperbolic intersection with the ocean surface. Therefore, an analysis based on a plane N-wave approximation is valid over a small region of the incident wavefront.

In this section, the theory of plane sinusoidal wave reflection, transmission and penetration at a plane air-water interface is reviewed. The similar available theory for the special case of an incident plane N-wave is then summarized. Finally, the limitations of existing theories in providing useful predictions for realistic situations are outlined.

2.2 PLANE SINUSOIDAL WAVES

The theory of the reflection, transmission and penetration of incident plane sinusoidal (single-frequency) wavefronts at a plane air-water interface is well established.[2] The plane wave is assumed to propagate in the direction of the normal to the wavefront.

Two physical boundary conditions must be satisfied across the interface. The acoustic pressure and the normal component of fluid particle velocity must be continuous across this boundary.

The critical angle for transmission of energy across the air-water interface, measured as the inclination of the acoustic ray from the

vertical, or as the angle between the acoustic wavefront and the horizontal interface, is about 13^{o}.

For angles of incidence less grazing than this, acoustic energy from the incident wavefront is partially reflected from the surface, and partially transmitted into the water as a propagating acoustic wavefront.

For angles of incidence more grazing than the critical angle, there is total reflection of the incident acoustic energy from the air-water interface. There is no propagating acoustic wavefront in the water, but there is penetration of sound into the water in the form of nonpropagating inhomogeneous wave. The amplitude of this penetrating sound pressure field dies out exponentially with depth, as a function of frequency. The inhomogeneous wave sweeps through the water horizontally at the same speed as the incident wavefront sweeps across the ocean surface. This speed of advance is less than the speed of sound in the water.

Because the acoustic impedance of water is greater than that of air, the reflected wave is in phase with the wave which is incident upon the air-water interface. For the case of total reflection, the amplitude of the reflected wave is equal to that of the incident wave. Together with the physical requirement that the acoustic pressure be continuous across the boundary, this means that there is "pressure doubling" across the interface. The amplitude of the penetrating pressure field just under the surface is double that of the incident acoustic wavefront in the air just above the surface.

The acoustic skin effect just described is significant only at very low frequencies. For example, at 10 Hz, the skin depth (depth at which the pressure amplitude is reduced by a factor of 1/e, or about 8.5 db)

is of the order of 10 feet, and at 1 Hz, it is of the order of 100 feet. But this very low frequency region is just the band in which most of the acoustic energy due to sonic booms is concentrated.

2.3 PLANE N-WAVES

The theory of total reflection of a plane N-wave from a plane air-water interface, with the accompanying penetration of a nonradiating pressure field in the water, has recently been developed.[3,4,5] Only the case of incidence of an N-wave at an angle more grazing than the critical angle has been considered. This case is relevant to the penetration of sonic boom energy into the ocean due to horizontal flights of supersonic aircraft at speeds up to the speed of sound in water, roughly Mach 4.5.

2.3.1 Scope of Existing Theory

A small region of the sonic boom shock cone at any point along the hyperbolic intersection of the cone with the ocean surface is treated in the existing theories. The angle of incidence of a shock cone wavefront region at the hyperbolic intersection ranges from a minimum value equal to the Mach angle of the shock cone, occurring at the vertex of the hyperbola, to a maximum value of 90°, occurring at the cutoffs of the hyperbolic intersection.

Neither of the theorists who have to date considered the problem of penetration of sonic booms into the water have put together the effects which occur over small regions of the incident shock cone, to describe the total overall phenomenon.

However, the radius of curvature at any point along the hyperbola is large compared to the thickness of the sonic boom shock cone. Also, the penetrating pressure field in the water is nonradiating. Thus, the composite sonic boom penetration effect is likely to involve smooth transitions between results obtained in individual regions along the hyperbolic intersection.

2.3.2 Sound Pressure Amplitude as a Function of Depth

The problem of determining the penetrating sound pressure field as a function of depth for an incident plane N-wave has been solved through a Fourier transform approach. The Fourier transforms of the two-dimensional wave equation and the traveling pressure N-wave at zero depth in the water are taken. The transformed wave equation is solved in the frequency domain, subject to the boundary conditions of the transform of the N-wave at zero depth and the requirement that the solution for the pressure remain bounded as the depth becomes infinite. The resulting solution is then inverse Fourier transformed back to the time domain.

Using the notation of Sawyers,[4] the results may be summarized as follows. The N-wave in the water at zero depth is

$$p(x,0,t) = \begin{cases} 0 & \text{for} \quad (t + x/v) < 0; \\ p_o \left[1 - (2/T)\right](t + x/v) & \text{for } 0 \le (t + x/v) \le T; \\ 0 & \text{for} \quad T < (t + x/v), \end{cases} \qquad (2\text{-}1)$$

where x is horizontal distance, t is time, v is the horizontal speed of advance of the N-wave in the water at zero depth, p_o is the peak pressure of the N-wave in the water, and T is the duration of the N-wave.

The waveform at depth z is given by Sawyers as

$$p(x,z,t) = (p_o/\pi)\, \varsigma \left\{ \left[(\tau/\varsigma) + ((\tau-1)/\varsigma) \right] \times \left[\text{Arctan}\,((\tau-1)/\varsigma) - \text{Arctan}\,(\tau/\varsigma) \right] + \left[\ln\left(1 + (\tau/\varsigma)^2\right) - \ln\left(1 + ((\tau-1)/\varsigma)^2\right) \right] \right\} \qquad (2\text{-}2)$$

in which, for brevity, $\tau = (t + x/v)/T$ is a normalized time- and-horizontal-distance variable, and $\varsigma = (1 - v^2/c^2)^{1/2}\, z/vT$ is a normalized depth variable. In the latter expression, c is the speed of sound in the water.

The results obtained by Sawyers are shown in Figure 2-1, for normalized depths of $\varsigma = 0^+$, 0.01, 0.1 and 0.5. This figure shows the

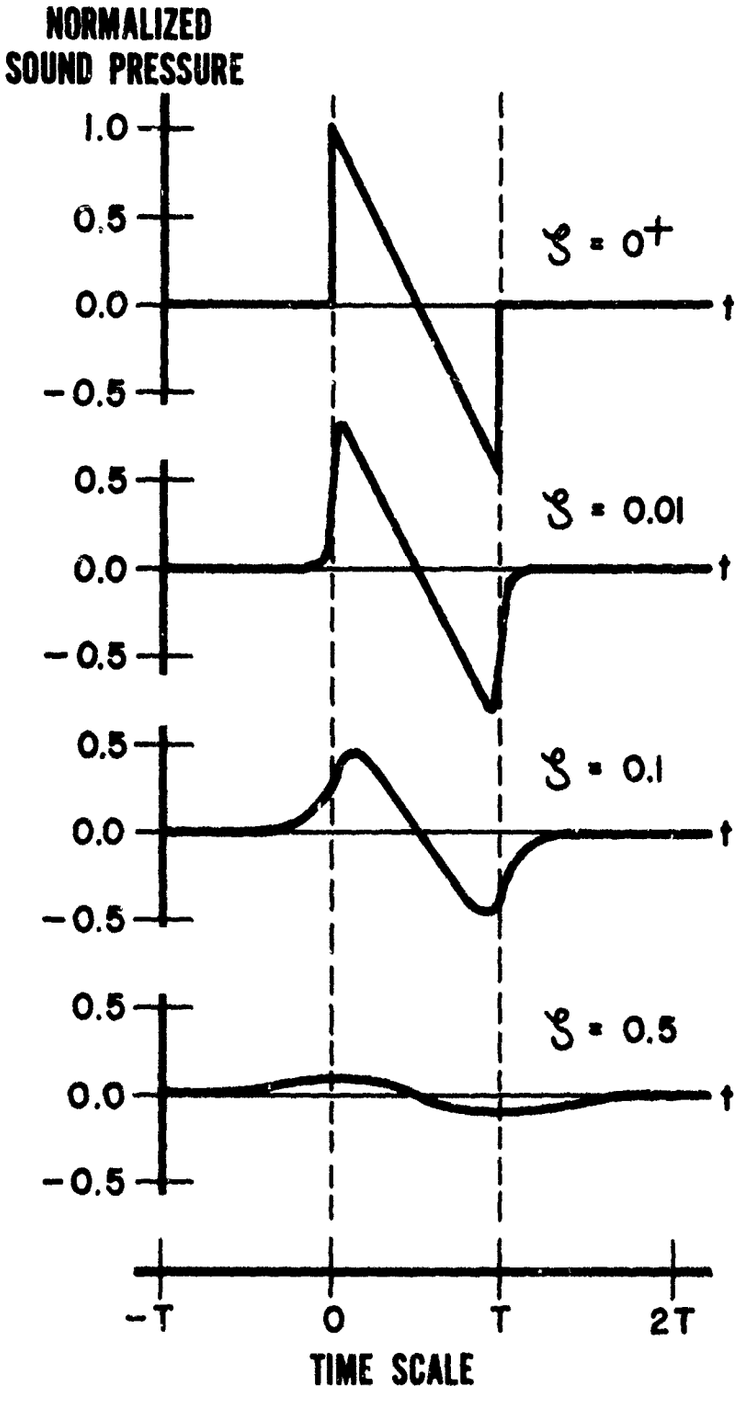

Figure 2-1. Theoretical Pressure Waveforms for Penetration of N-Wave Into Water

time waveforms which would be seen by fixed sensors at x = 0, at the various depths. For typical values of v = 1500 ft/sec, c = 4800 ft/sec and T = 0.1 sec, the actual depths corresponding to the indicated values of ζ would be 0^+, 2, 16 and 80 ft, respectively.

The waveforms shown in Figure 2-1 become more rounded and extended as the depth increases. The infinitely long precursors and tails have odd symmetry about t = T/2. This result is what would be expected if, as indicated in the previous discussion of plane sinusoidal waves, the higher frequencies were attenuated more rapidly than the lower frequencies as a function of depth. The effect is that of a low-pass filter.

In a more recent investigation, Cook[5] has obtained the same result as that given in Equation 2-2, plus an additional term. The additional term has even symmetry about t = T/2, with infinite spikes at t = 0 and t = T, and another precursor-tail pair. However, Cook indicates that this additional term usually makes a negligible contribution to the total sound pressure, and will be difficult to measure.

It must be noted in the foregoing discussion, that p_o is the peak pressure of the N-wave in the water. This is twice the peak pressure of the incident N-wave in the air just above the air-water interface. As discussed earlier, this pressure doubling is a consequence of the in-phase total reflection of the incident wave, and the physical requirement of continuity of acoustic pressure across the interface.

2.3.3 Energy Density Spectrum as a Function of Depth

The expression for pressure as a function of depth, given in Equation 2-2 and plotted in Figure 2-1, is rather complicated. It is easier to estimate the effects of variations in depth in terms of the energy density spectrum of the N-wave.

The N-wave energy density spectrum as a function of depth, z, is given[3] by the square of the modulus of P(x, z, f), which is the Fourier transform of the pressure amplitude, p(x, z, t):

$$Q(z,f) = 2\,p_o^{\,2}\,T^2\,F(2\pi T f)\exp(-(4\pi/m)\,z\,f) \qquad (2\text{-}3)$$

where $m = (1 - v^2/c^2)^{-1/2}\,v$ and where

$$F(\theta) = (1 + \cos\theta)/\theta^2 - 4\sin\theta/\theta^3 + 4(1 - \cos\theta)/\theta^4 \qquad (2\text{-}4)$$

is the normalized two-sided N-wave energy density spectrum[6] defined on the interval $(-\infty, +\infty)$.

Equation 2-3 shows that a signal component at frequency f decreases exponentially in amplitude with increasing depth. If the frequency at which the energy density spectrum peak occurs is approximated as $f_o = 1/2T$, then the skin depth, z_o, for which the amplitude of the dominant frequency decreases by a factor of e^{-1} is roughly $z_o = vT/\pi \approx L/\pi$. In the latter expression, $L = vT$ is the thickness of the sonic boom shock wave in the direction of advance.

The two-sided energy density spectrum given in Equation 2-4 is useful theoretically, but since it involves negative frequencies, it is not consistent with physically measurable quantities. For purposes of comparing theoretical predictions with experimental measurements, the one-sided energy density spectrum defined on the interval $(0, +\infty)$ must be used.[7] The one-sided energy density is double the two-sided energy density. If the expression given in Equation 2-3 is to represent a set of physically measurable values, it must be multiplied by a factor of two.

2.3.4 Comparisons of Sonic Boom and Ambient Spectra

To determine whether sonic boom energy which penetrates into the ocean to a given depth will be detectable in the midst of noises from other sources, some measure of the amplitude of the sonic boom signal must be compared with a similar measure of the ambient noise amplitude.[3]

A detailed comparison of relative pressure levels as a function of frequency can be obtained by comparing the sonic boom and ambient sound pressure spectrum levels. Spectral components of the sonic boom can be detected in frequency regions where the sonic boom level is appreciably higher (at least 6 db) than the ambient level.

Ambient spectra are generally presented in terms of sound pressure spectrum levels, with a 1 Hz reference bandwidth.[8] Thus, a power density spectrum is used for ambient noise. If the detailed power density spectrum values were known over bandwidths much less than 1 Hz, the sound pressure spectrum levels would be obtained by integrating the power density spectrum values over 1 Hz frequency bands. In practice, however, only the sound pressure levels in bands larger than 1 Hz are measured, and these measurements are converted to a 1 Hz basis.

The theoretical sonic boom spectra described in the previous section were energy density spectra. These must first be converted to power density spectra, before comparisons between sonic boom and ambient spectra can be made.

A power density spectrum may be constructed for the sonic boom pressure field by dividing the energy density spectrum by the duration of the incident N-wave, T. This definition of a sonic boom power density spectrum is less than satisfactory at depths greater than $z = 0^+$, where the duration of the pressure waveform exceeds T. However, it does make possible a comparison of sonic boom and ambient spectra on the same basis, in the same physical units.

2.4 SUMMARY

The sound pressure waveform at depth z due to an incident plane N-wave having peak pressure p_I in air is given by Equation 2-2, in which $p_o = 2\, p_I$.

The sonic boom sound pressure spectrum level at depth z is given by

$$L(z,f) = 10 \log_{10} \left\{ 16 p_I^2 \; T \; F(2\pi Tf) \exp(-(4\pi/m)\, zf) \right\} \qquad (2\text{-}5)$$

where p_I is the peak pressure of the incident N-wave in air, in units of 0.0002 dyne/cm^2, and where the notation is otherwise the same as in Equation 2-3. The units of L(z, f) are db//0.0002 dyne/cm^2, for convenient comparison with published ambient levels. The above expression for L(z, f) differs from that which would be obtained by converting Equation 2-3 to decibels, in three respects.

(1) The peak pressure p_o in the water at the surface has been replaced by $p_I = p_o/2$, where p_I is the peak incident pressure in the air, to account for pressure doubling across the interface;

(2) The two-sided energy density spectrum Q (z, f) has been replaced by a physically measurable one-sided energy density spectrum, S (z, f) = 2 Q (z, f);

(3) A power density spectrum has been constructed by dividing the energy density spectrum by the duration, T, of the incident N-wave.

The net effect of these modifications is to change the expression for the sonic boom pressure spectrum derived by Sawyers (Ref. 3, Equation .1) by a factor of 8/T. The sonic boom pressure spectrum so obtained is suitable for comparison with physical measurements of ocean ambient noise.

2.5 LIMITATIONS

The presently available theory of the penetration of sonic booms into the ocean is limited by the following set of assumptions:

(1) The aircraft is in horizontal flight in a given direction at constant speed over an extended interval of time;

(2) The aircraft speed is less than the speed of sound in water (about Mach 4.5).

(3) The ocean surface is flat, and the ocean itself is homogeneous throughout;

(4) Results apply only to small regions of the intersection of the Mach cone with the ocean surface, where the plane wave approximation is valid;

(5) Only symmetrical N-waves, having zero rise times and linearly changing pressure amplitudes, are involved.

Although these assumptions are rather restrictive, the theory which has been developed on this basis is appropriate for application to operational situations of current interest.

Section 3

DESCRIPTION OF EXPERIMENT

3.1 PURPOSE OF EXPERIMENT

The purpose of the experiment was to measure the penetration of acoustic energy into water from a simulated sonic boom. An explosive charge was detonated in the air over a small body of water. The resulting spherically spreading shock wave simulated a region of a sonic boom incident upon the surface of the water, as shown in Figure 3-1.

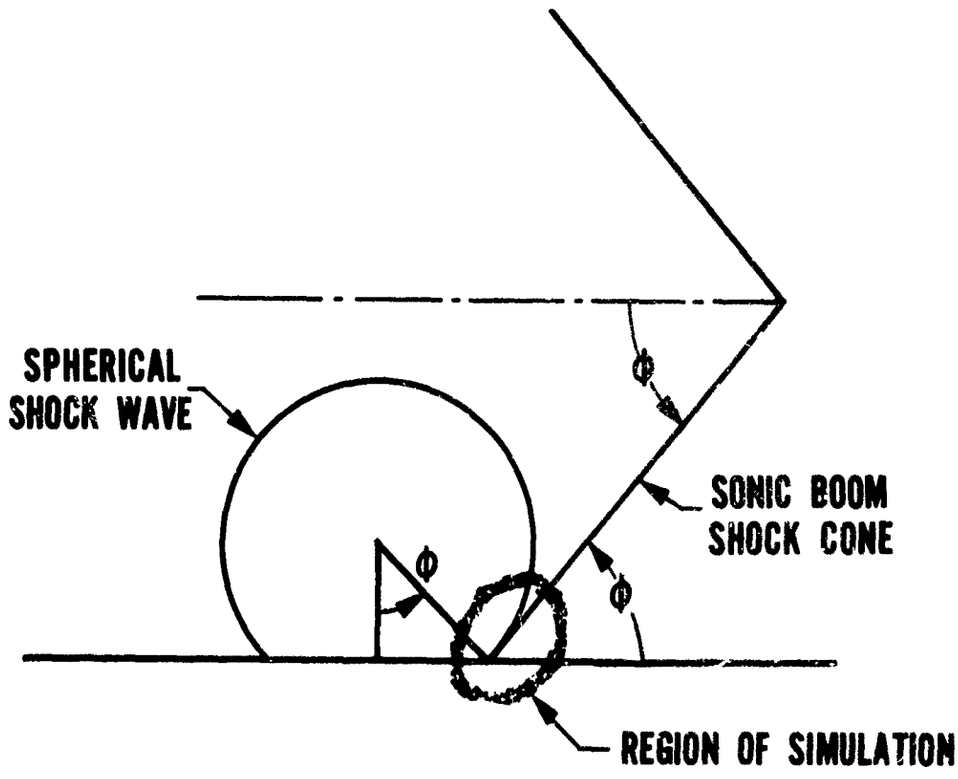

Figure 3-1. Simulation of Region of Sonic Boom Shock Cone, Using Portion of Spherical Shock Wave

3.2 ARRANGEMENT OF INSTRUMENTATION

The overall geometry is shown in Figure 3-2. The small body of water was a flooded quarry, 300 ft wide and 80 ft deep. The explosive charge was suspended from a high horizontal cable. Two arrays of sensors were suspended in the area from a low horizontal cable. A local array, consisting of a microphone and hydrophone, was fixed directly under the explosive charge. A movable remote array, consisting of a microphone and three hydrophones, was positioned at various distances from the local array.

Signals from the two arrays were brought to amplifiers in an electronics hut aboard a barge about 50 ft from the local array. The signals were then brought up to a control shack on shore, where they were recorded on magnetic tape and on a light-beam oscillograph. The explosive charges were detonated on command from the control shack.

3.3 EXPLOSIVE CHARGES

The explosive charges used to produce spherical shock waves were 6-grain dynamite blasting caps. These charges were emplaced in groups of six and were detonated singly, using a 12-volt auto battery and long electrical leads.

The dynamite caps were placed at a height of 30 ft above the water. A typical shock waveform as measured by the local microphone, at a height of 3.8 ft above the water, is shown in Figure 3-3. The pressure waveform produced by the dynamite cap was a good approximation to an ideal N-wave. The negative pressure portion of the actual waveform had about 0.8 of the peak amplitude and about 1.3 of the duration of the positive portion.

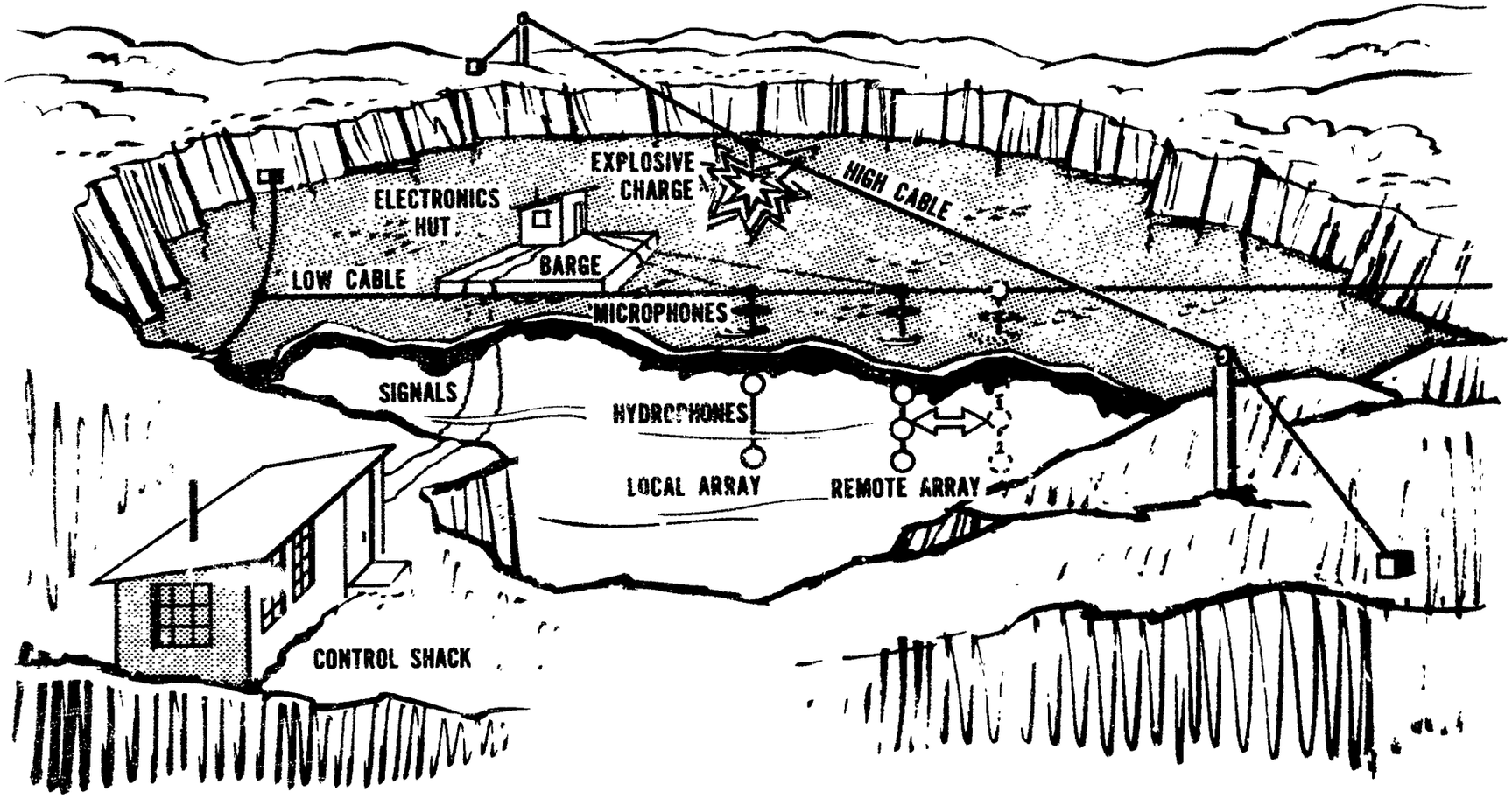

Figure 3-2. Geometry of Sonic Boom Simulation Experiment

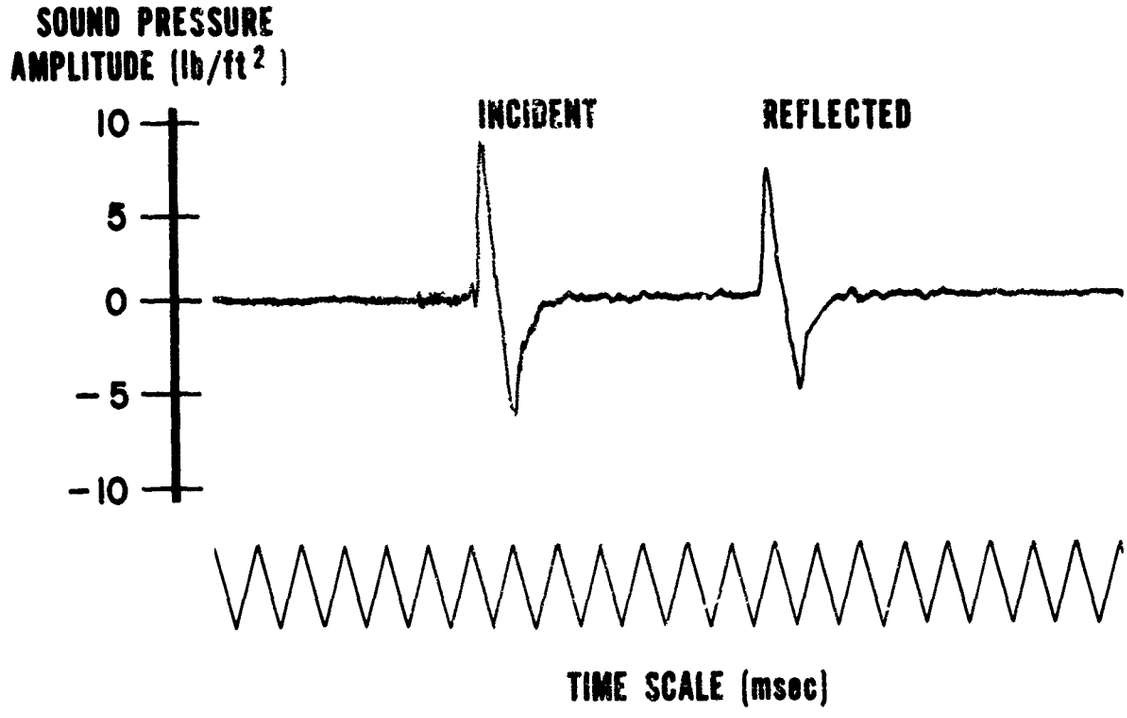

Figure 3-3. Airborne Pressure N-Wave Due to 6-Grain Dynamite Cap

Both the incident and reflected signal components of the airborne shock wave near the water surface are shown in Figure 3-3. The amplitude of the reflected component was about 0.78 that of the incident component. This was due principally to spherical spreading, since the incident wave was almost completely reflected even in the case of near-normal incidence. The distance along the direct path from the source to the receiver was 26.2 ft, and the reflected path distance was 33.8 ft.

At a distance of about 50 ft from the dynamite cap, which was a typical placement of the remote array in the experiment, the peak sound pressure amplitude was about 5 lb/ft^2, and the duration of the N-wave was about 1.5 msec. Thus, the dynamite cap successfully simulated the order of magnitude of the peak pressure of a sonic boom (typically 2.5 lb/ft^2). However, the duration of the N-wave due to the dynamite cap was two orders of magnitude less than that due to a sonic boom (typically 0.1 to 0.3 sec).

Because the duration of the simulated sonic boom N-wave was about 1% of that of a real sonic boom, the predicted penetration in the experiment was also only about 1% of that which would actually occur. But this amount of penetration, of the order of one foot in the experiment, did prove to be measurable. In retrospect, it is clear that if N-waves having durations of 0.1 to 0.3 sec had been used in the experiment, no meaningful measurements could have been made because of reverberations in the small body of water which was used. It would have been necessary to conduct the experiment in the deep ocean, which would have been a much more ambitious undertaking.

The 6-grain dynamite caps were reasonably consistent in the production of similar peak sound pressure amplitudes from one shot to the next. The maximum variation during one series of 26 shots was about $\pm$ 30%.

3.4 MICROPHONES

The two microphones used to measure signals at the air side of the air-water interface were special sonic boom sensors, provided for use in the experiment by NASA/Langley. These were carrier systems, consisting of Photocon Model 464 condenser microphone and coil combinations which formed tuned circuits.[9] These systems had good frequency response from roughly 0.1 Hz to 10 kHz. This was more than adequate for the experiment, since the spectra of the N-waves measured in the experiment probably peaked at about 500 Hz. The systems also had good dynamic range; sound pressure amplitudes as great as 10 lb/ft^2 could be measured with linear response.

3.5 HYDROPHONES

The four hydrophones used to measure signals in the water were Wilcoxon Series 50 and 70 units, provided for use in the experiment by the U. S. Navy. These hydrophones had reasonably good low-frequency response, down to at least 10 Hz. Each unit had a preamplifier built in next to the hydrophone element, providing good gain against electrical noise pickup on the signal cable. Each unit also had provision for insertion of a system calibration signal into the hydrophone preamplifier.

3.6 MAGNETIC TAPE RECORDING

The signals from the two microphones and four hydrophones were recorded on magnetic tape, using an Ampex FR-1300 14-channel recorder. The signals were recorded in the FM mode at 30 ips, to provide a frequency response of 0 to 10 kHz. Additional signals recorded with the acoustic signals included the dynamite cap firing signal, a 1000-Hz sawtooth timing signal, and voice annotations.

3.7 OSCILLOGRAPH RECORDING

A 7-channel Consolidated Electrodynamics Corporation light-beam oscillograph was used to provide permanent records of the acoustic signals,

all displayed on a common time base. The oscillograph was used to monitor the acoustic signals on-line during the experiment. It was also later used in the laboratory, for further analysis of the signals played back from the magnetic tape. For this purpose, the tape recordings were in some cases slowed down by a factor of 4 on playback, to provide better time resolution on the oscillograph displays.

3.8 CALIBRATION OF SYSTEM

Proper calibration of each of the six acoustic data channels was an essential part of the experiment. Different methods were used for the calibrations of the microphone and hydrophone data channels.

The microphones were calibrated in place before and after the series of shots, using a single-tone, 1 kHz acoustic signal level of 150 db//0.0002 dyne/cm^2, rms. This signal had a peak sound pressure amplitude of about 18.6 lb/ft^2, which was of the order of magnitude of the largest peak airborne pressure amplitude measured in the experiment. The known calibration signal was fed into the microphones using a special calibrator supplied with the microphones by NASA/Langley.

Each microphone data channel consisted of a carrier microphone system with discriminated analog voltage output, a postamplifier, a magnetic tape unit (recording and immediately replaying signals on-line), an oscillograph galvanometer driver amplifier, and an oscillograph signal display channel. The calibration consisted of measuring the amplitude of deflection of the oscillograph trace for the known input sound pressure amplitude, for each microphone data channel. When actual data was acquired during the experiment, any changes in the gain settings from those used during calibration were noted.

The hydrophone data channels, exclusive of the hydrophone crystals, were calibrated in place before and after the series of shots, using a single-frequency 1 kHz electrical signal amplitude of 1 volt, rms.

This voltage was typical of the output of the hydrophone crystal in response to the largest peak underwater pressure amplitude measured in the experiment.

Each hydrophone data channel consisted of a hydrophone crystal, preamplifier, postamplifier, attenuator pad, magnetic tape unit, oscillograph driver amplifier, and oscillograph signal display channel. The electrical calibration signals were fed into the preamplifiers.

To complete the calibration of the hydrophone data channels, the sensitivities of the hydrophone crystals were measured in a separate experiment, which was conducted following the sonic boom simulation experiment. The hydrophone crystal sensitivities were measured both by the reciprocity calibration method and by use of 1 kHz tone bursts from a calibrated projector at a known distance. The results of the latter calibration were checked by calibrating hydrophones of known sensitivities along with the unknowns. Details of the hydrophone calibration measurements are given in Reference 10.

The 1 kHz frequency used in the calibrations of the acoustic sensors was of the order of magnitude of the frequency range which contained most of the acoustic energy of the 1.5 msec N-wave signals used in the experiment.

It is estimated that absolute pressure amplitude measurements made with the microphones were accurate to within $\pm$ 1 db, and that absolute measurements made with the hydrophones were accurate to within $\pm$ 2 db. The calibrations were believed to be good down to at least 1 Hz for the microphones, and down to at least 20 Hz for the hydrophones. The upper cutoff frequency for all acoustic measurements made in the experiment was about 10 kHz, because of the magnetic tape recorder.

Section 4
SUMMARY OF EXPERIMENTAL RESULTS

4.1 OPTIMUM GEOMETRY

On the basis of Sawyers' theoretical expression for the penetration of an acoustic N-wave into the water (Equation 2-3), the penetration depth for an N-wave of 1.5 msec duration was predicted to be a few feet. An effort was made to place the three hydrophones of the movable remote array at depths of 1, 2 and 4 ft. However, due to the catenary in the cable from which the remote array was suspended, the actual depths of the hydrophones in the remote array were one or two ft greater than intended, for the array locations which gave the best results in the experiment.

About 20 shots were made with the remote array positioned at various horizontal distances between 15 and 145 ft from the local array, which was placed directly under the explosive charge. The height of the explosive charge above the water was 30 ft for all shots in the series.

The optimum geometry for measurement of penetration of acoustic energy from the incident shock wave was one in which the remote array was 25 to 60 ft from the local array. The reason for this was interference due to other transmitted (rather than penetrating) signal component arrivals.

Figure 4-1 shows the location of sensors for two shots in which the geometry was good for making measurements of sound penetration into the water under total reflection conditions. The rays of sound within the critical angle which were transmitted across the air-water interface into the water are shown. In the figure, these rays were constructed at 5^{o} increments in the water, using Snell's Law. The wavefronts and their times of arrival are also shown at equally spaced intervals of time in the figure. The instant at which the spherically spreading airborne

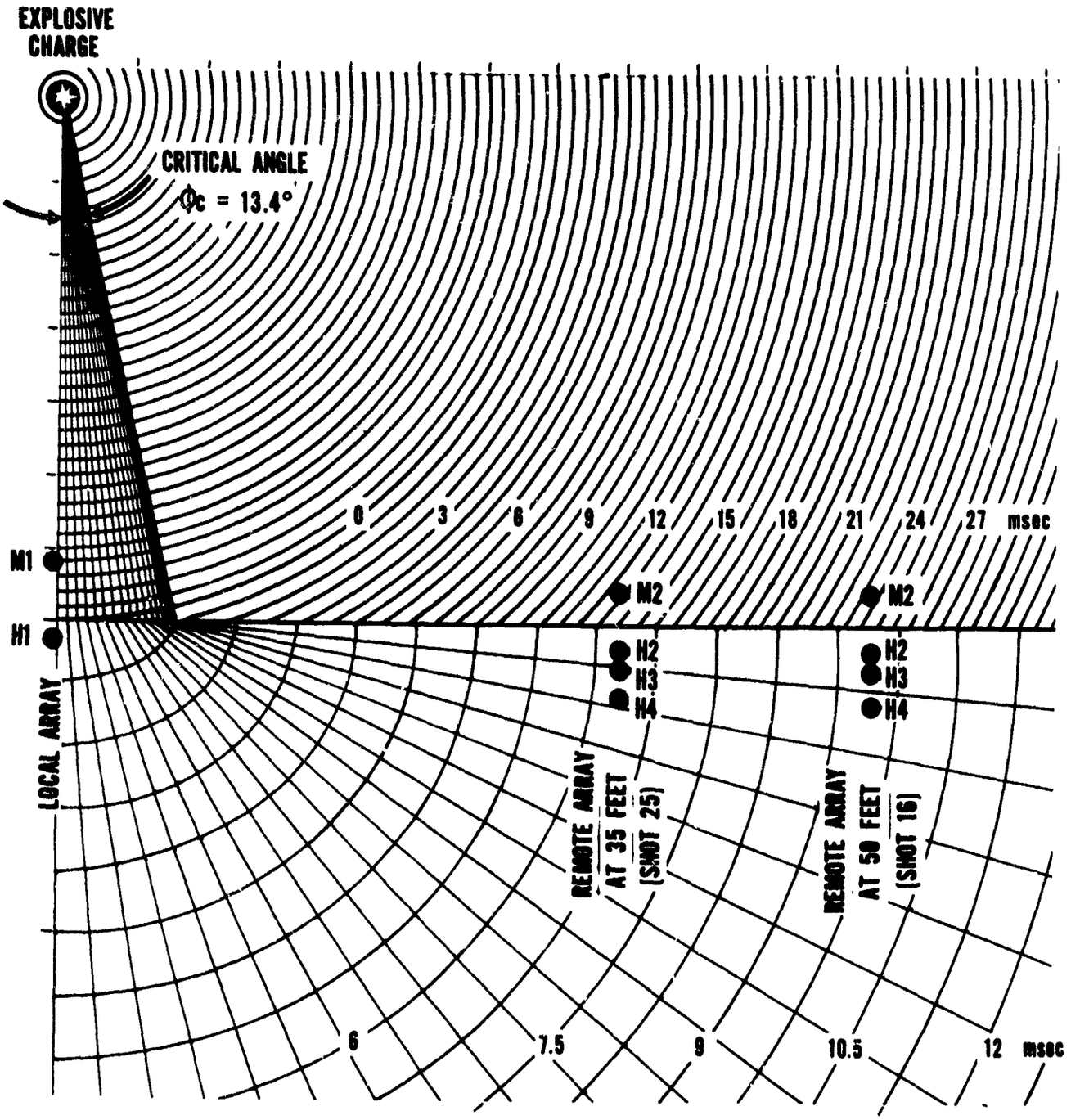

Figure 4-1. Locations of Sensors for Measurements of Penetration of Shock Wave Energy into Water

shock wave first reaches the water directly below the explosive charge is taken as time t = 0.

Figure 4-1 was useful for the prediction of the times of arrival of the transmitted and penetrating signal components at the hydrophones of the remote array, as a function of its distance from the local array. For Shot 25, the remote array was 35 ft from the local array. The transmitted signal component was expected to arrive at t = 6 msec, and the penetrating signal component at 13 msec. For Shot 16, at 50 ft, the transmitted signal component was expected at t = 9 msec and the penetrating signal component at t = 24 msec. In making these estimates, it was assumed that the time of arrival of the penetrating signal at the remote hydrophones was the same as the time of incidence of the shock wave on the water surface vertically overhead, as predicted by Sawyers' theory.[4]

When the remote array was positioned at 10 to 25 ft from the local array, the transmitted and penetrating signal components arrived at the remote hydrophones at nearly the same time (3 msec apart at 25 ft). Also, when the remote array was more than about 60 ft away from the local array, the penetrating signal arrived at the remote hydrophones at the same time as reverberations from the bottom and walls of the rock-lined quarry. Thus, there was an optimum geometry of remote array locations at 25 to 60 ft from the local array. This optimum geometry provided a "window" through which the penetration of sound into the water could be measured without interference from other transmitted signal components.

The speed of advance of the shock wavefront across the water surface in the optimum geometry ranged from about 1200 to 1700 ft/sec, or from about Mach 1.1 to Mach 1.6. The corresponding angles of incidence ranged from about 63° to 40°.

4.2 REFLECTOR-ABSORBER

It was recognized that it would be desirable to increase the width of the penetration measurement "window" provided by the optimum geometry just described. An effort was made to prevent that portion of the shock wavefront which would be transmitted across the air-water interface from reaching the water. To do this, a plane reflector-absorber was constructed to block out acoustic rays within the 13.4^{o} cone shown in Figure 4-1.

The reflector-absorber was built of plywood, 16 ft square, and covered with 3 in of sound absorbing urethane foam. It was suspended over the water directly under the explosive charge, tilted slightly from the horizontal, about 6 feet above the water. At this height, with the explosive charge 30 feet above the water, the diameter of the 13.4^{o} cone to be blocked out was less than 12 ft.

The sound pressure amplitudes due to successive shots were measured at the undisturbed local microphone before and after the reflector-absorber was put in place. These measurements indicated that the reflector-absorber reduced the amplitude of the signal coming directly through it by a factor of about 10.

However, due to diffraction effects at the edges of the reflector-absorber, sound nevertheless entered the water around the reflector-absorber at angles of less than the critical angle, 13.4^{o}. The amplitude of this diffracting sound was not appreciably less than that of the sound which had previously gone into the water directly, without the reflector-absorber. The sound which was diffracted around the reflector-absorber and transmitted into the water caused, if anything, more interference with the desired measurement of the penetration phenomenon.

There appeared to be no simple way to avoid the diffraction effect, short of building outward-sloping skirts all around the reflector-absorber, right to the surface of the water. Further use of the reflector-absorber in the experiment was therefore abandoned.

4.3 USE OF FLOATS

In the early stages of setting up the experiment, floats were used to hold up the local and remote arrays, rather than overhead cables. The floats were fully inflated automobile inner tubes.

In the analysis of the on-line oscillograph records from a series of preliminary shots, spurious signal components were observed which could not be identified either as components transmitted as in Figure 4-1, or as penetrating components. The spurious signal components always arrived after the components due to direct transmission, and arrived later at the deep hydrophone than at the shallow one.

It was suspected that the spurious signal components were caused by the floats used to hold up the arrays. Figure 4-2 shows the signals received at the local microphone and at two rather deep remote hydrophones for one particular shot made when the floats were present. The remote array was about 30 ft from the local array. The local microphone was 3 ft above the water, and the remote hydrophones were at depths of 23 and 53 ft.

Under these conditions, the direct transmitted signal components should have arrived at the 23 and 53 ft hydrophones at 7.7 and 12.8 msec, respectively. Any signal components which were transmitted into the water by the float supporting the remote array should have arrived at the same hydrophones at 11.3 and 17.7 msec, respectively. Figure 4-2 shows that the measured signal components indeed occurred roughly as anticipated. The components associated with the float occurred several milliseconds later than expected, if anything. (In preparing the oscillograph record for Figure 4-2, the playback system gains were purposely set high, so that the direct transmission signal component would be clipped, while the signal component due to the float would be easily seen.)

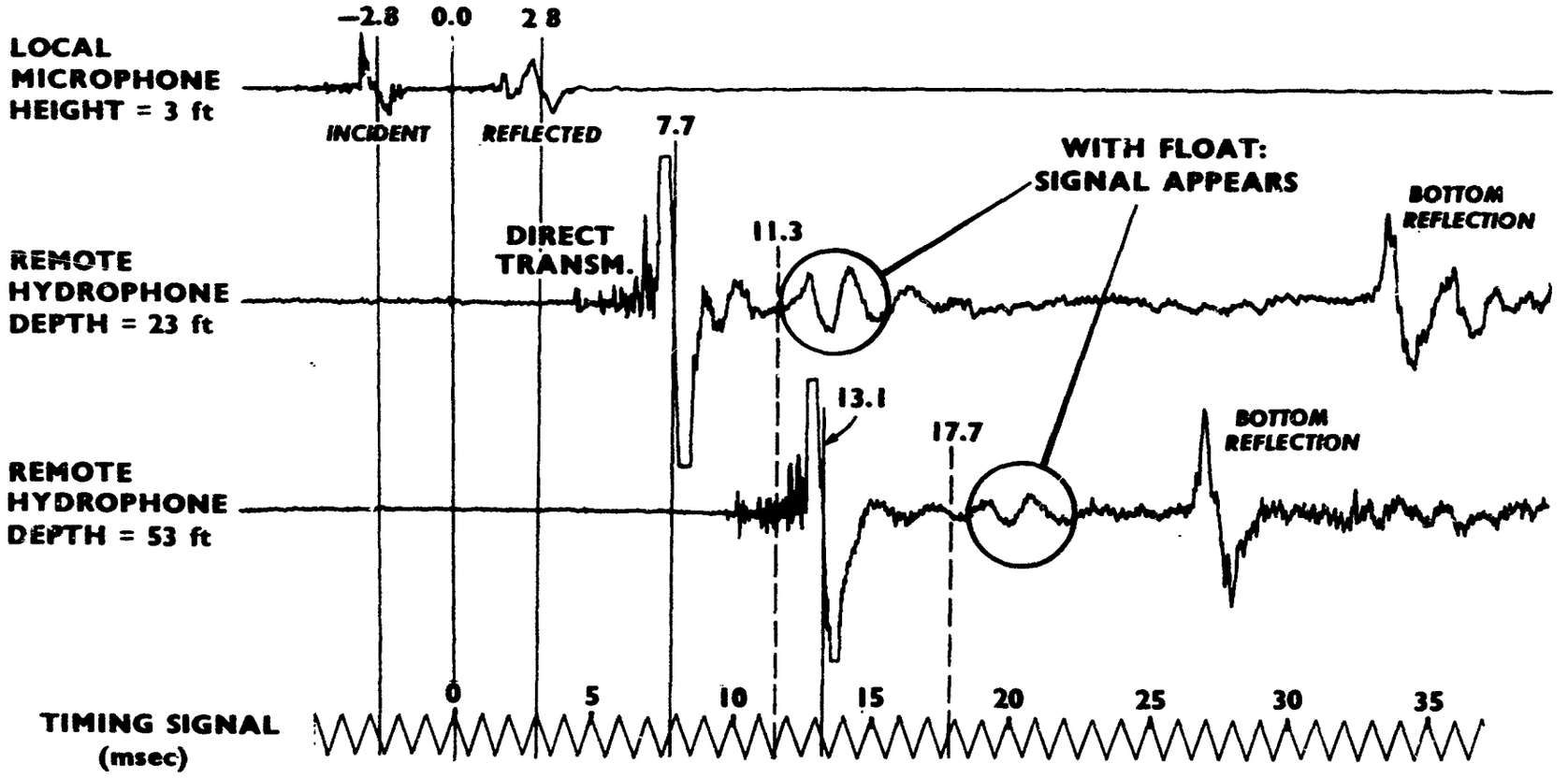

Figure 4-2. Transmission of Shock Wave Sound Into Water due to Presence of Float

It was confirmed that the spurious signal components were caused by the floats, by making another shot in which the floats were removed. The local and remote arrays were suspended from overhead steel cables for this shot, in the same positions as when the floats were present. The results are shown in Figure 4-3. The signal components at about 13 and 20 msec for the 23 and 53 ft hydrophones, respectively, which were present when the floats were present, were not observed with the floats removed.

As a result of this experience, it was concluded that the float above the remote array was being excited by the incident airborne snock wave and was reradiating sound directly into the water. This sound transmitted into the water did not attenuate rapidly with distance. Since the floats introduced signals which interfered with the desired measurement of penetration of sound under total reflection conditions, the floats were removed. All subsequent experimental work was done without any floats.

4.4 RESULTS FOR SELECTED MEASUREMENTS

The experimental results for two selected measurements of penetration of shock wave energy into the water are shown in Figures 4-4 and 4-5. These shots were made with the optimum geometry, and with no floats in the water. The surface of the water was flat for all shots.

Four distinct events are identified in these figures. The first event was the initial incidence of the spherically spreading shock wave upon the water. This event defined time t = 0, which was halfway between the times at which the incident and reflected pulses were sensed at the local microphone. The second event was the arrival of transmitted acoustic energy at the remote hydrophones along a path such as indicated earlier in Figure 4-1. The third event, which was of principal interest in the experiment, was the arrival of the airborne shock wave at the remote

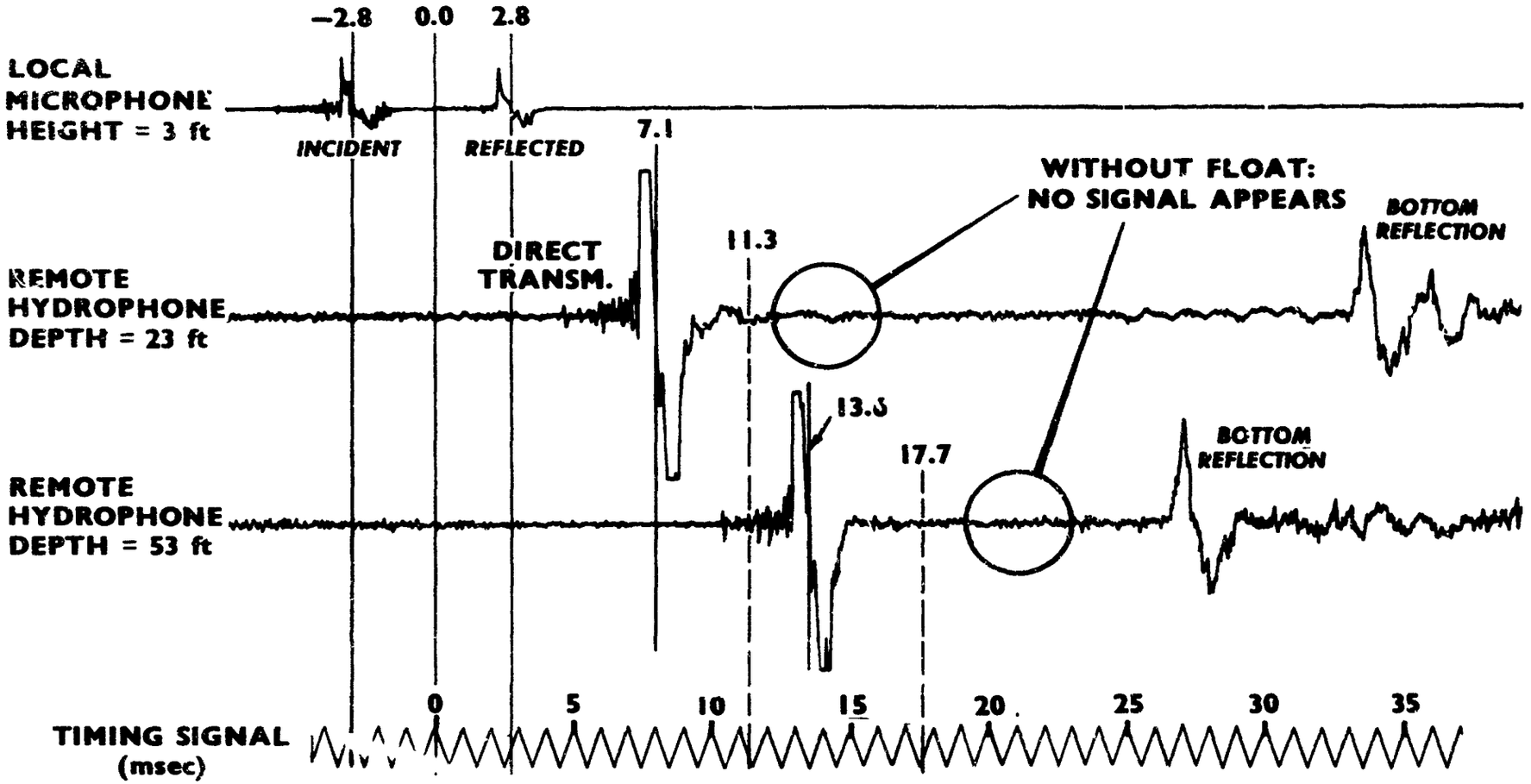

Figure 4-3. Signals Received with Same Geometry as for Figure 4-2, But Without Float

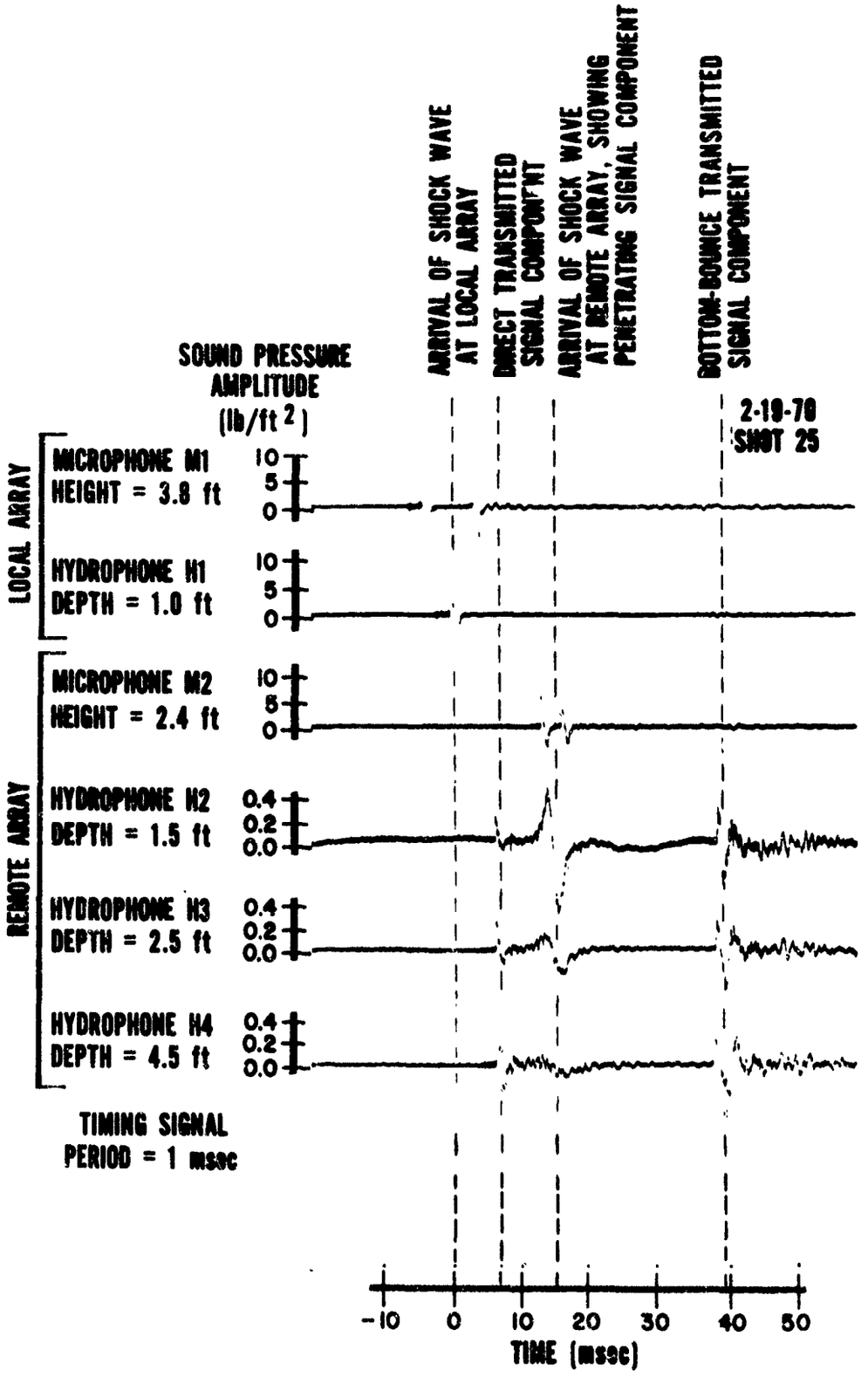

Figure 4-4. Oscillograph Record for Shot 25, With Remote Array 35 ft from Local Array

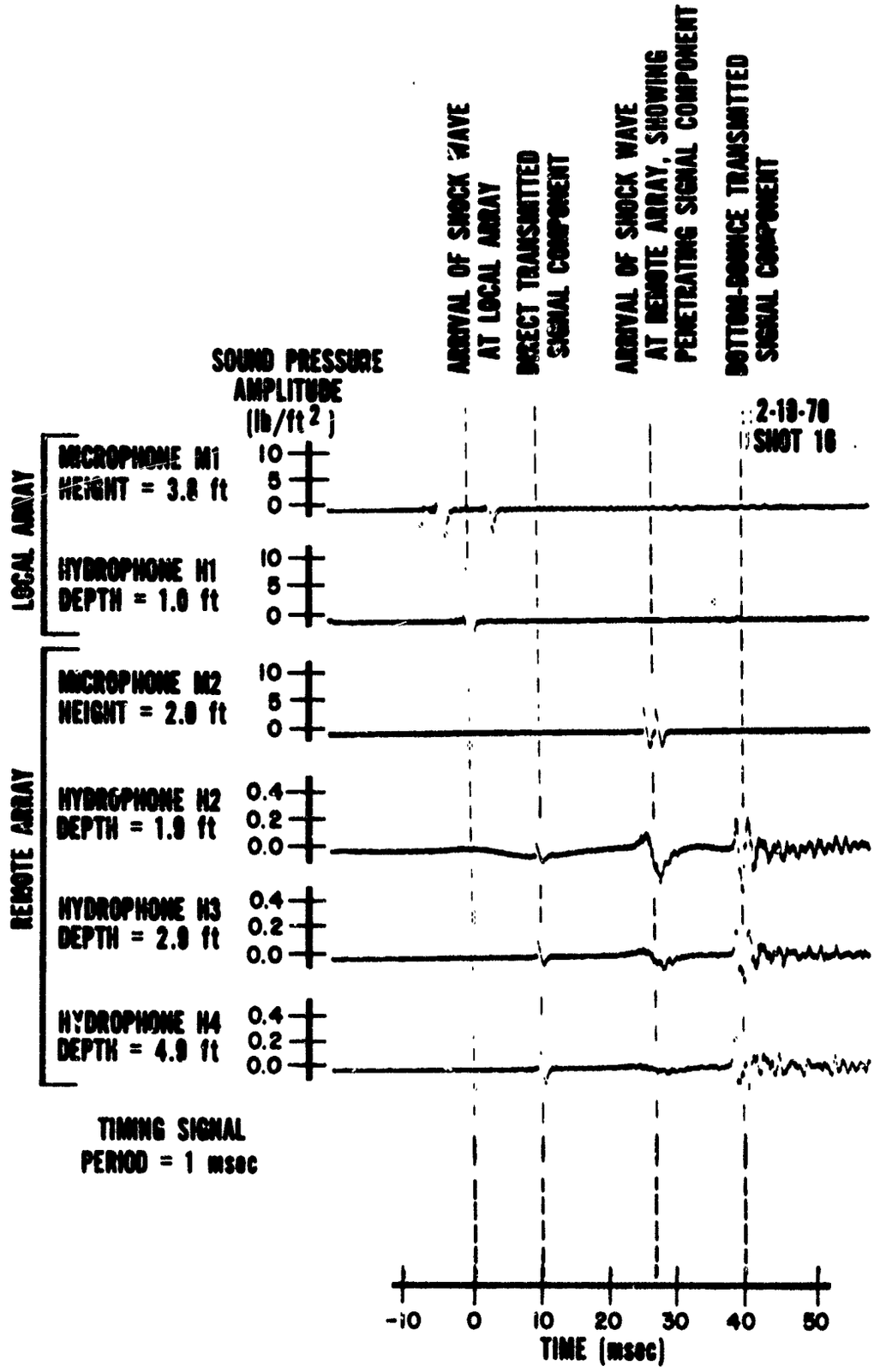

Figure 4-5. Oscillograph Record for Shot 16, With Remote Array 50 ft from Local Array

microphone, and the penetration of acoustic energy into the water as sensed by the remote hydrophones. The fourth event was the arrival of transmitted acoustic energy at the remote hydrophones along the shortest of the bottom-bounce paths.

On the basis of Figure 4-1, the predicted times of occurrence of the second and third events for Shot 25 were 6 and 13 msec, respectively. For Shot 16, the corresponding predicted times were 9 and 24 msec.

Figure 4-4 shows that the measured times of occurrence of the second and third events for Shot 25 were actually 7 and 15 msec, respectively. For Shot 16, Figure 4-5 shows that the corresponding measured times were 10 and 27 msec. These measured times were 10 and 27 msec. These measured times were consistently about 10% greater than the predicted times. This indicates that the measurements of distance made during the experiment were not too accurate. Also, the local array may have been displaced by several feet from the point directly under the dynamite cap.

The peak amplitude of the transmitted sound pressure pulse sensed by the local hydrophone positioned at a depth of 1 ft directly under the local microphone was about equal to the average of the peak amplitudes of the incident and reflected airborne waves. At zero depth, the pulse in the water should have had double this amplitude. However, the local hydrophone was not at zero depth, and it was probably not exactly under the explosive charge. Under these conditions, air-to-water sound transmission theory[11, 12] indicates that a geometric spreading loss of as much as 6 db is quite possible.

The direct transmitted signal components received at the remote hydrophones decreased in amplitude with depth. This was also in accord with the predictions of air-to-water sound transmission theory.[11, 12] Very little acoustic energy is transmitted nearly parallel to the air-water interface.

Figures 4-4 and 4-5 show that there was indeed penetration of shock wave energy into the water under total reflection conditions. The amplitude decreased rapidly with depth, and there was a rounding of the initial waveform with depth. The measured behavior was generally that predicted by the existing theories, as summarized in Section 2.

4.5 COMPARISONS WITH THEORETICAL PREDICTIONS

4.5.1 Detailed Comparisons for Selected Measurements

Figures 4-6 and 4-7 provide detailed comparisons between the theoretical predictions and experimental measurements for the two shots discussed in the previous section. The theoretical curves are those computed from Equation 2-2. In evaluating p (0, z, t) for comparison with an experimental measurement, the values of ζ, τ and p_0 used in Equation 2-2 were based on the measured hydrophone depth, z; incident N-wave duration T; and incident N-wave peak pressure, p_I. Peak pressure p_0 at z =0 in the water was taken to be equal to $2p_I$, where p_I was measured at the remote microphone.

For the penetration of sound measured in Shot 25, shown in Figure 4-6, the horizontal speed of advance of the shock wave across the water at the point of measurement (35 ft from the local array) was about 1460 ft/sec, or about Mach 1.32. For Shot 16, shown in Figure 4-7, the speed of advance was about 1290 ft/sec, or about Mach 1.18.

The agreement between the theoretically predicted and experimentally measured detailed waveforms was quite good, within a factor of two in both the amplitude and time scales.

4.5.2 Summary of Peak Amplitudes

Table 4-1 provides a comparison between the theoretically predicted and experimentally measured peak pressure amplitudes for eight shots made with the remote array at distances ranging from 25 to 60 ft from the

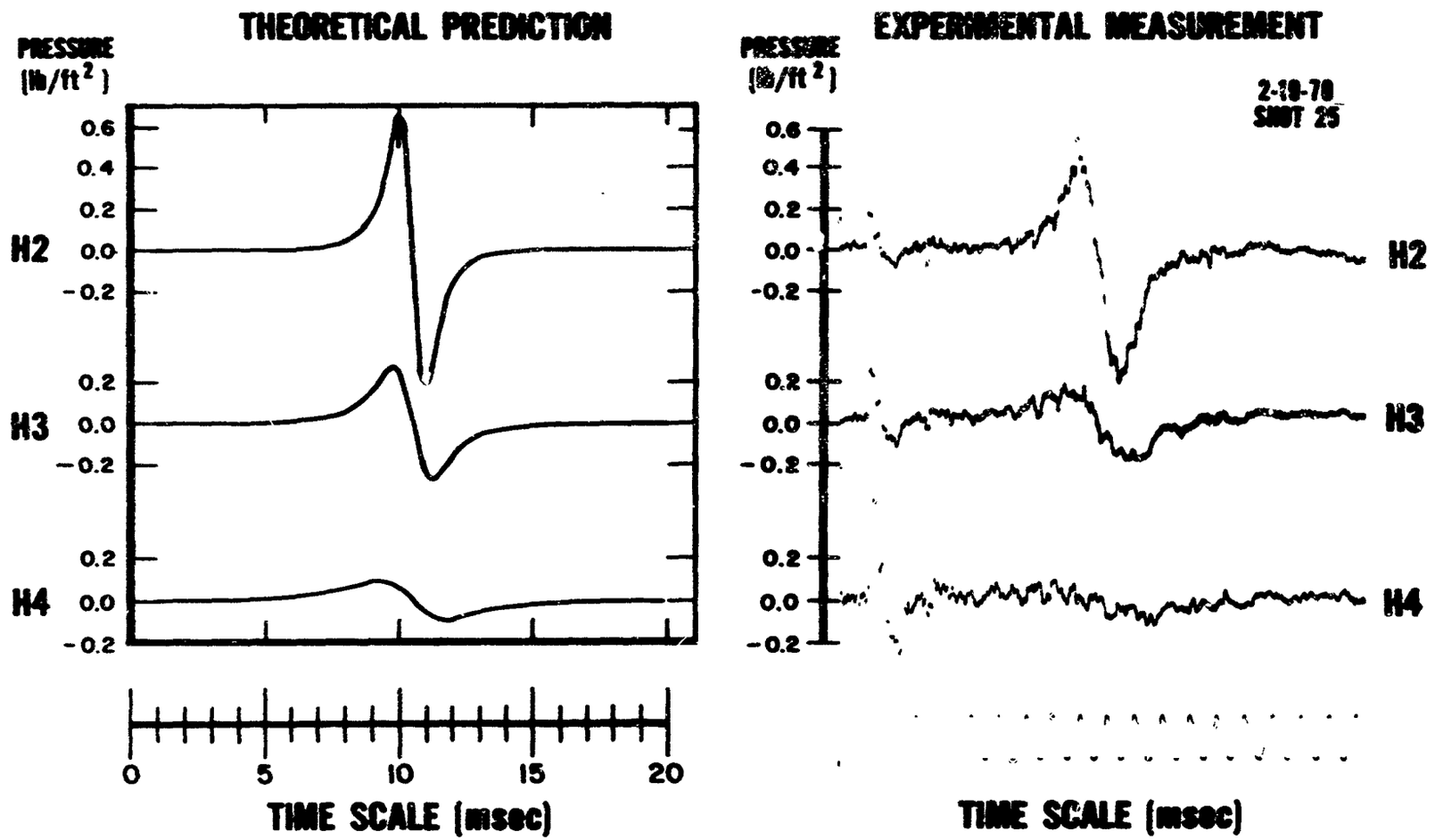

Figure 4-6. Comparison between Theoretical Prediction and Experimental Measurement of Penetration of Shock Wave Energy into Water: Shot 25

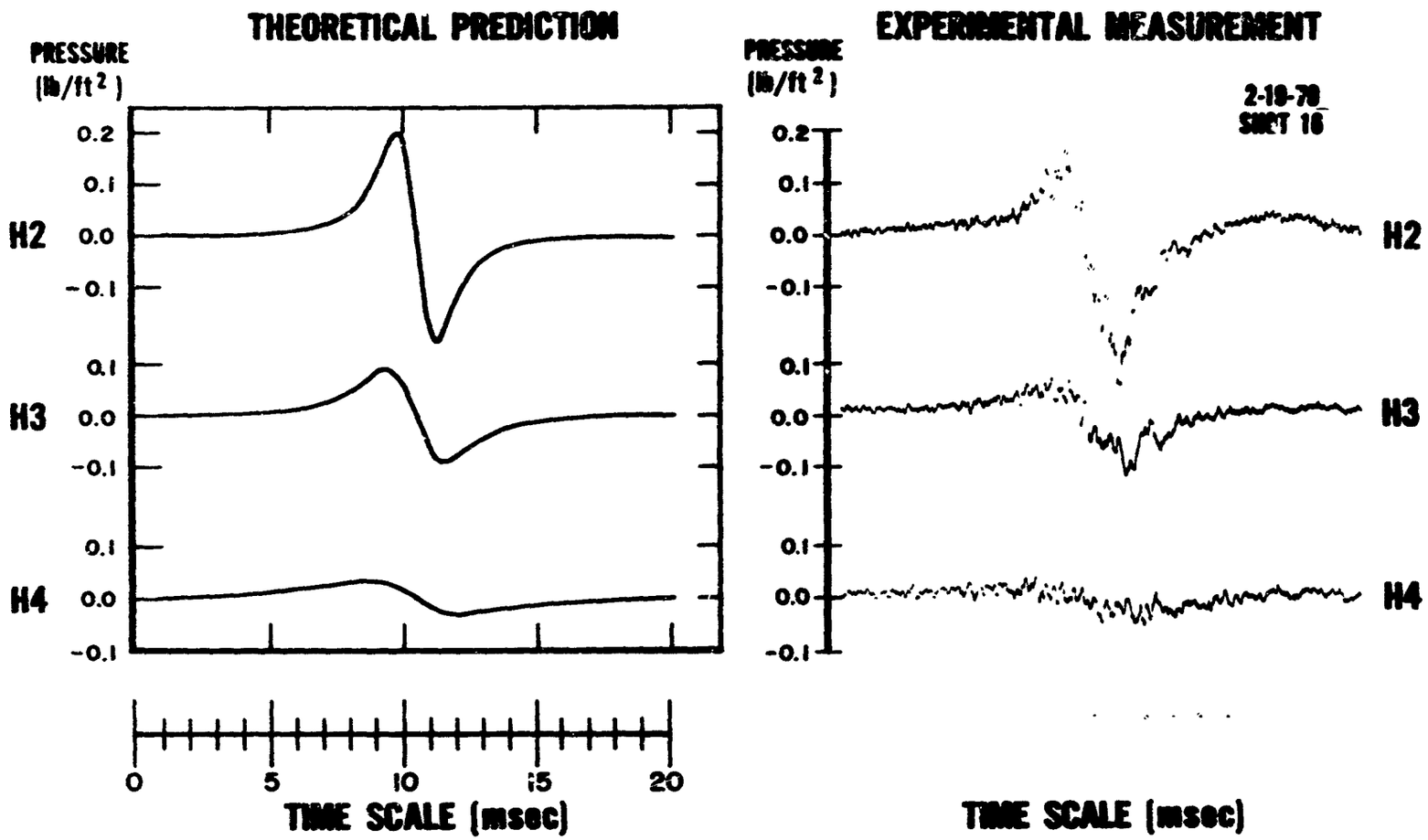

Figure 4-7. Comparison between Theoretical Prediction and Experimental Measurement of Penetration of Shock Wave Energy into Water: Shot 16

Table 4-1. Summary of Peak Amplitudes

Shot Number	Distance (ft)	Mach Number	Measured p_I (lb/ft^2)	Measured T (msec)	Depth (ft)	Peak Pressure Amplitude (lb/ft^2) Measured	Predicted
12	25	1.66	6.2	1.22	1.2	0.78	1.63
					2.2	0.22	0.63
					4.2	0.10	0.19
13	30	1.41	5.6	1.42	1.3	0.56	0.78
					2.3	0.16	0.29
					4.3	0.06	0.09
14	35	1.32	5.9	1.54	1.5	0.29	0.28
					2.5	0.11	0.11
					4.5	0.07	0.03
15	40	1.25	5.3	1.54	1.6	0.28	0.46
					2.6	0.07	0.19
					4.6	0.04	0.06
6	45	1.20	5.4	1.42	1.7	0.18	0.37
					2.7	0.08	0.16
					4.7	0.04	0.05
16	50	1.17	4.2	1.50	1.9	0.16	0.21
					2.9	0.04	0.09
					4.9	0.02	0.03
17	55	1.14	3.1	1.46	2.0	0.12	0.13
					3.0	0.03	0.06
					5.0	0.02	0.02
18	60	1.12	3.9	1.43	2.1	0.19	0.39
					3.1	0.05	0.19
					5.1	0.02	0.07

local array. Measurements were made at depths in the 1 to 5 ft region. This series of shots covered horizontal speeds of advance ranging from Mach 1.12 to Mach 1.66.

Equation 2-2 was used to provide theoretical predictions of the peak pressure amplitude as a function of depth, for a shot having the same values of incident N-wave peak pressure amplitude, duration, and speed of advance as those measured in the shot. The general agreement between measured and predicted amplitudes was rather good; the predicted amplitudes were usually higher. In several cases, the presence of appreciable low-frequency (around 200 Hz) noise made accurate measurements of peak pressure amplitudes difficult. This low-frequency noise also made it generally difficult to identify the extent of precursors and tails in the experimental measurements.

Section 5

PENETRATION OF SONIC BOOM ENERGY INTO THE OCEAN

5.1 INTRODUCTION

The previous two sections have described an experiment in which measurements were made of the penetration of acoustic energy into a body of water from a portion of an airborne shock wave, which swept across the water in the manner of a sonic boom. The portion of the shock wave which was involved in this experiment closely resembled a sonic boom in peak pressure amplitude, angle of incidence and waveshape, but had a duration which was about 0.01 that of a typical sonic boom. Thus, the depths of penetration of energy from the shock wave into the water in the experiment were about 0.01 as great as would occur for an actual sonic boom incident upon the ocean surface.

The measurements made in this acoustically scaled experiment were in good general agreement with predictions based on the existing theory of N-wave penetration into the ocean under total reflection conditions. As a result, it may be assumed that the theory is valid, within the restrictions imposed by the simplifying assumptions on which the theory is based.

5.2 COMPARISONS WITH AMBIENT NOISE LEVELS

It is of interest to assess the possible ecological consequences of the penetration of sonic boom acoustic energy into the ocean. To do this, theoretically predicted sonic boom underwater sound levels must be compared with the deep-ocean ambient noise levels which are normally present. This is best done as a function of frequency, by comparing sound pressure spectrum levels.

Sawyers[3] has previously compared predicted sonic boom spectrum levels at a depth of 15 ft with ambient noise spectrum levels, for two representative cases. The purpose of the present work is to incorporate several modifications to Sawyers' approach, and to expand the comparison over a greater range of data.

For convenience, the same two cases considered by Sawyers will be discussed. In Case 1, the N-wave duration is taken as T = 0.1 sec, and the aircraft speed is v = 1500 ft/sec. In Case 2, T = 0.3 sec and v = 2500 ft/sec. In both cases, a peak pressure amplitude of p_o = 2.5 lb/ft^2 and a speed of sound in water of c = 4800 ft/sec are assumed.

Figure 5-1 shows the sound pressure spectrum levels for the airborne sonic boom N-waves incident upon the ocean surface, for Cases 1 and 2. These pressure spectrum levels differ from the energy density spectra usually discussed in the literature[6] by factors of 2/T, or 13 db and 8 db for Cases 1 and 2, respectively. The modification provides sound pressure spectrum levels which are directly comparable with physically measurable ambient spectrum levels.

Figures 5-2 and 5-3 provide comparisons between theoretically predicted sonic boom spectra at 0, 15, 100 and 1000 ft depths and measured deep-ocean ambient spectra, over frequencies ranging from 0.01 to 10,000 Hz.

The predicted spectra were computed from Equation 2-5, discussed in Section 2-4 of this report. At the 15-ft depth, the predicted spectra of Figures 5-2 and 5-3 are higher than those shown by Sawyers (Reference 6, Figure 1) by a factor of 8/T, which is 19 db and 14 db in Cases 1 and 2, respectively.

The "typical" ambient spectra[8,13] in Figures 5-2 and 5-3 are for heavy surface ship traffic and Sea State 3. Over frequencies from 1 to 10,000 Hz, the "upper limit" and "lower limit" spectra[8] are the same as these shown by Sawyers. The typical spectrum for transient ambient noise due to earthquakes and explosions[8] is also shown, since this is relevant to sonic boom transient noise in the ocean.

There are four important physical sources[8] of typical ambient noise in the deep ocean, for a frequency range of 0.01 to 10,000 Hz.

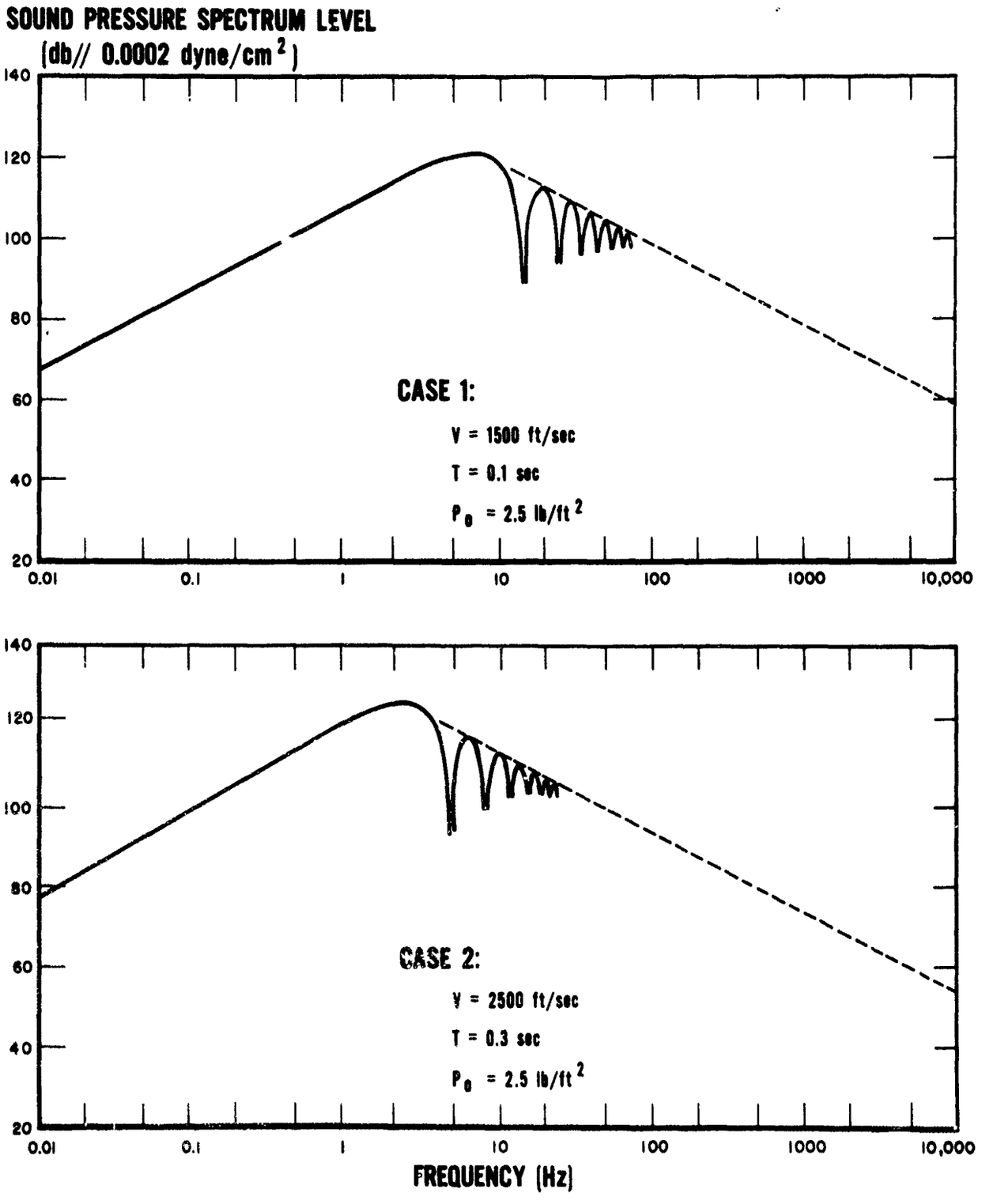

Figure 5-1. Sonic Boom Sound Pressure Spectrum Levels in Air at Surface of Water, for Two Cases

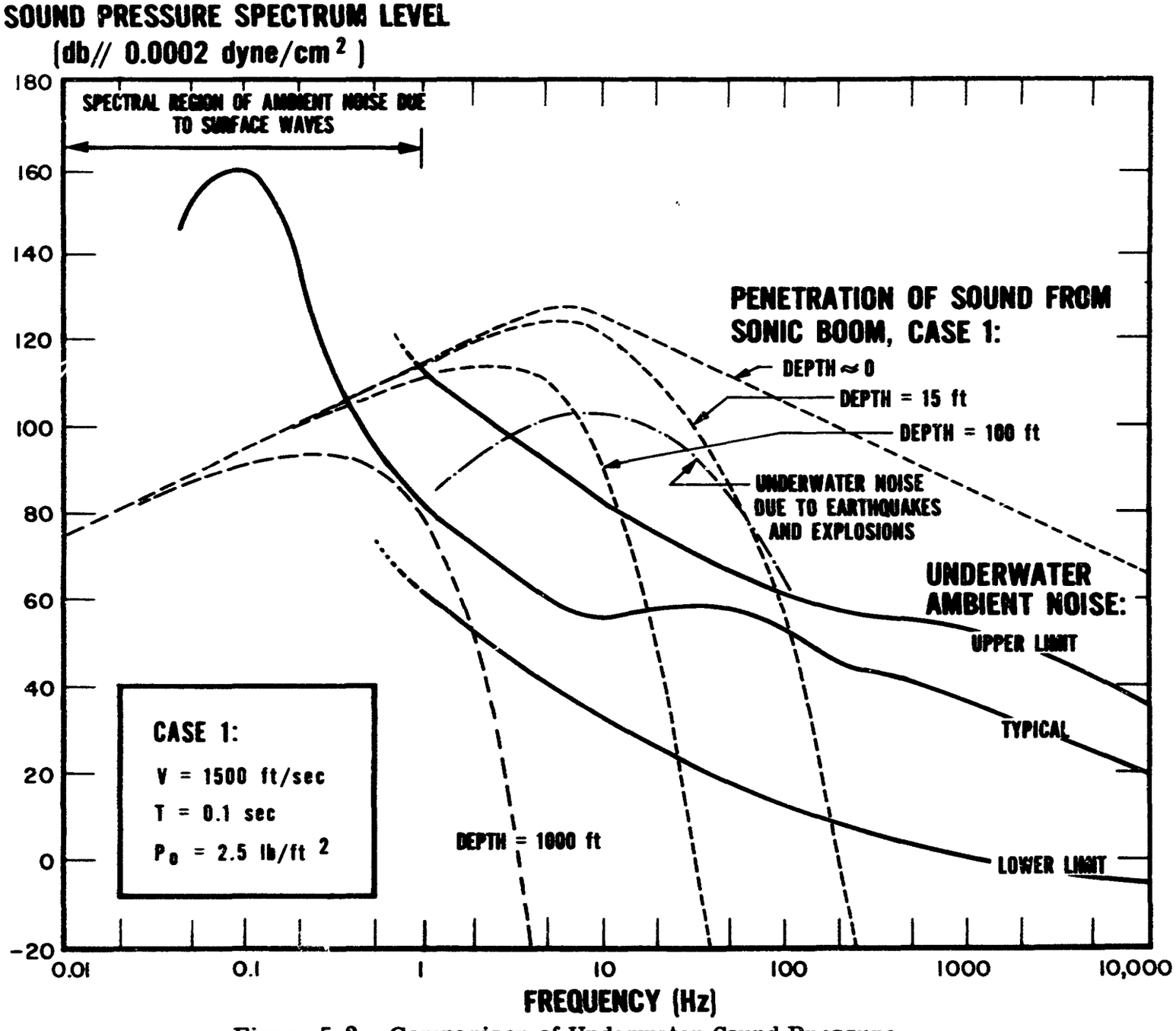

Figure 5-2. Comparison of Underwater Sound Pressure Spectrum Levels for Sonic Boom and Ambient Noise: Case 1

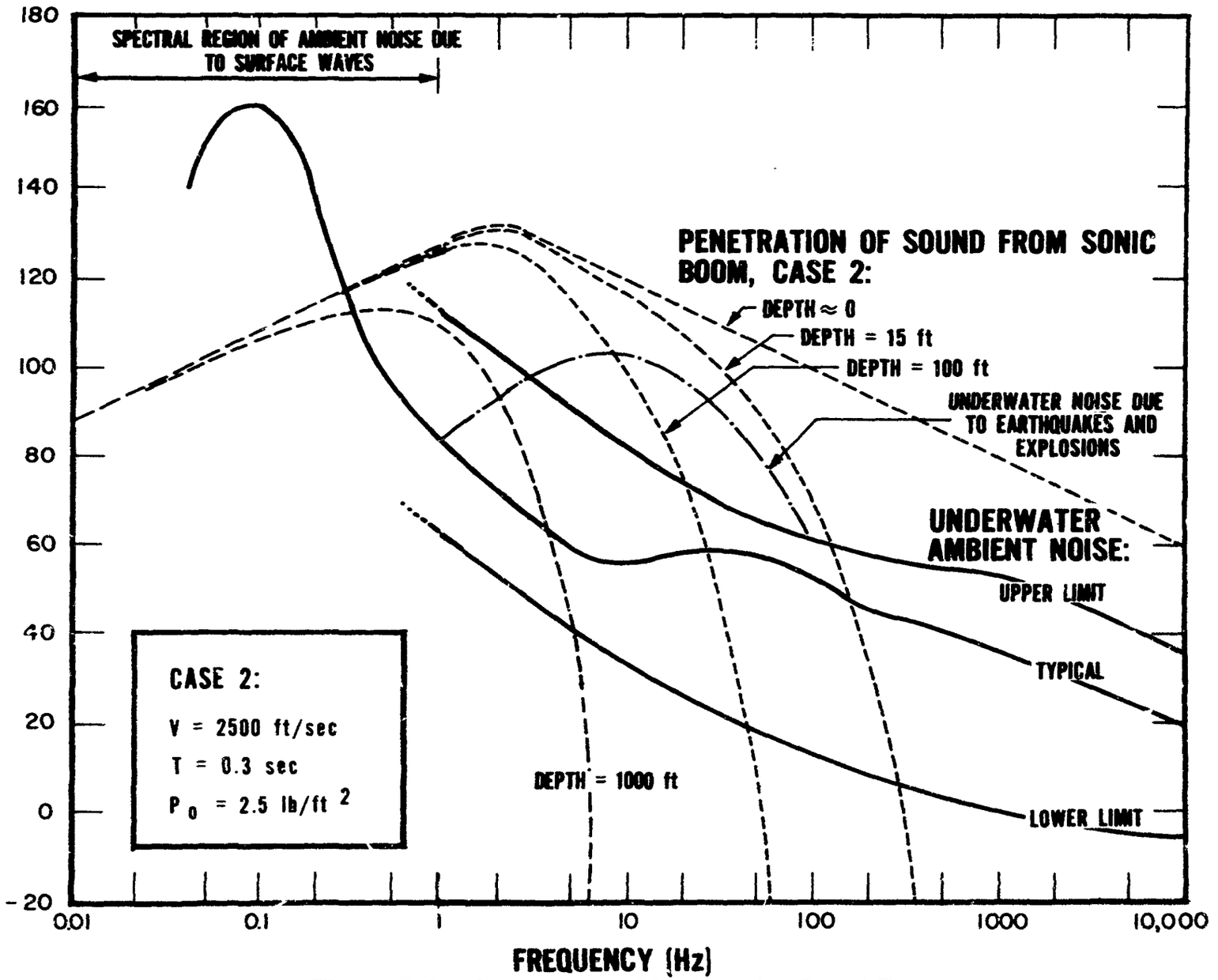

Figure 5-3. Comparison of Underwater Sound Pressure Spectrum Levels for Sonic Boom and Ambient Noise: Case 2

Figures 5-2 and 5-3 show that the underwater noise levels due to sonic booms penetrating into the ocean to depths of 15 ft or more appreciably exceed the naturally occurring ambient noise levels only in the very low frequency region from about 0.5 to 200 Hz. The penetrating sonic boom spectra have peaks in the region from about 0.5 to 5 Hz. These spectral peak levels exceed the corresponding typical ambient levels by about 60 db at a depth of 15 ft and by about 50 db at 100 ft. At depths of more than a few thousand ft, the sonic boom noise level does not appreciably exceed the ambient noise level at any frequency.

The sonic boom spectral peaks occur in roughly the same frequency region as the peaks of transient ambient noise due to earthquakes and explosions. The peak levels of the sonic boom spectra are 20 to 30 db higher than the peaks of the low-frequency transient ambient noise spectra.

Although the predicted peak levels of the penetrating sonic boom noise spectra are well above the ambient noise levels in the region from 0.5 to 5 Hz, these sonic boom levels are well below the ambient noise spectrum levels in the 0.1 Hz region. This is the region in which surface waves cause ambient pressure fluctuations. For a well-developed Sea State 3, the ambient noise spectrum levels at 0.1 Hz are 30 to 40 db above those at 0.5 to 5 Hz due to penetration of sonic booms into the ocean.

5.3 EQUIVALENT SURFACE WAVES

The amplitude of the pressure fluctuations due to penetration of a sonic boom into the ocean may be expressed in terms of the height of an equivalent surface wave which causes pressure fluctuations of the same amplitude. At a depth of 15 ft, the pressure fluctuation amplitude associated with the penetration of a 2.5 lb/ft^2 incident sonic boom shock wave is 3 to 4 lb/ft^2, depending on the duration of the incident N-wave. A surface wavelet having a height of less than one inch is all that is needed to cause a pressure fluctuation of this amplitude at a point just beneath the surface, under the wavelet.

However, at a given frequency, the amplitudes of pressure fluctuations due to surface waves are attenuated exponentially with depth.[8] This occurs for surface waves for the same reason it occurs for sonic boom shock waves incident upon the surface. When pressure is applied from above upon a small region of the surface of a body of water such as the ocean, which is effectively unbounded to the sides and below, the pressure is carried by the water in all the horizontal directions as well as vertically. The amplitude of the pressure fluctuation goes to zero as the depth increases without bound.

At a frequency of 1 Hz, the amplitude of the pressure fluctuation due to a surface wave is reduced by a factor of about 0.0001 at a depth of 15 ft. This means that it would take a wave having a height of nearly 100 ft, with a period of 1 second, to cause a pressure fluctuation of 3 to 4 lb/ft^2 at a depth of 15 ft. Such waves do not exist. Thus, as indicated by Figures 5-2 and 5-3, the pressure fluctuations due to penetrating sonic booms at 15 ft are appreciably greater than the ambient pressure fluctuations.

At a frequency of 0.1 Hz, however, there is little attenuation of the surface wave pressure fluctuations at depths as great as 100 ft. This is why the ambient noise spectral peak appears at 0.1 Hz. There are also some second-order pressure variation effects which are not attenuated with depth.

5.4 PARTICLE DISPLACEMENTS

Using the plane-wave approximation, which is valid for a small region of an atmospheric sonic boom shock wave, the displacement experienced by an air particle as it is acted upon by the shock wave passing through is given by the time integral of the sound pressure, p (t), divided by the acoustic impedance, ρc. Here, ρ is the density of the medium, and c is the speed of sound in the medium.

In air, a sonic boom N-wave having a peak sound pressure amplitude of 2.5 lb/ft^2 and a duration of 0.1 sec will cause a particle displacement of about a quarter of an inch. A given air particle will be moved over this distance and then will be returned to its original position during the 0.1 sec interval, as the shock wave passes through. This effect is perceptible in the chest cavity of a human observer.

In water, the penetrating pressure field associated with a small region of the incident sonic boom also has the form of a plane wave. This inhomogeneous plane wave[2] is a vertical wavefront which moves horizontally through the water at the same speed as the incident sonic boom sweeps across the surface. At small depths, the peak sound pressure amplitude associated with this wavefront is roughly equal to that of the incident airborne shock wave. However, because the acoustic impedance of the water is about 3300 times that of air, the particle displacement will be much smaller in water than in air. At a depth of 15 ft, the penetrating sound pressure field due to the sonic boom described will cause a particle displacement of about one thousandth of an inch.

5.5 ECOLOGICAL CONSEQUENCES

In the present work, as in previous work,[3] it has been established that underwater pressure fluctuations due to sonic booms will be of higher amplitude than the deep-ocean ambient noise only in a very low-frequency region, and only at depths less than roughly a thousand feet. Further, it has been established that naturally-occurring pressure fluctuations due to surface waves have appreciably higher spectrum levels than penetrating noise due to sonic booms, even as shallow as 15 ft.

It remains for qualified biologists to determine the ecological consequences of the intrusion of transient pressure fluctuations at frequencies below about 200 Hz into the upper layers of the ocean. The available

evidence, including the very low-frequency nature of the sonic boom noise and the very small particle displacements involved, indicates that there will be little effect on the ocean ecology.

The crucial factor is the determination of the response of marine life to the stimulus of occasional pulses of low-frequency pressure fluctuations which are of larger amplitude than the ambient noise usually present.

Section 6
CONCLUSIONS

6.1 RESULTS OF EXPERIMENT

The experiment which was conducted was an acoustically scaled simulation of the penetration of sonic boom energy into the ocean. The experiment resulted in verification of predictions based on the existing theory of N-wave penetration into a flat body of water under total reflection conditions. Therefore, it is believed that the theory is valid, under the restrictions of the assumptions involved in its development.

6.2 COMPARISON WITH AMBIENT NOISE LEVELS

The sound pressure spectrum levels associated with the penetration of sonic booms to various depths in the ocean were computed, based on the theory. These predicted levels were compared with measured typical deep-ocean ambient noise spectrum levels over a wide range of frequencies. At depths of less than a thousand feet, the sonic boom levels were appreciably higher than the corresponding ambient noise levels only at very low frequencies, from about 0.5 to 200 Hz. The spectrum levels at about 0.1 Hz of ambient pressure fluctuations due to surface waves were appreciably higher than the sonic boom peak spectrum levels.

6.3 ECOLOGICAL CONSEQUENCES

The detailed ecological consequences of the penetration of sonic booms into the ocean remain to be determined by qualified biologists, based upon the quantitative predictions of spectrum levels developed by Sawyers[3] and in the present report. There are indications, however, that the ocean ecology will not be seriously affected by sonic booms.

6.4 SCOPE OF THEORY

The existing theory is limited in scope by a number of assumptions. The aircraft is assumed to be in horizontal flight at a constant speed,

less than Mach 4.5, over an extended interval of time. The ocean surface is assumed to be flat, and the ocean itself to be homogeneous. Results apply only to a small region of the intersection of the sonic boom shock cone with the ocean surface. Finally, only symmetrical N-waves with zero rise times and linearly changing pressure amplitudes are considered.

Despite the restrictive nature of these assumptions, the theory developed on this basis is believed to be appropriate for application to simple operational situations of current interest.

6.5 EFFECTS OF NONHORIZONTAL FLIGHT

So long as the supersonic aircraft does nothing to cause the sonic boom shock wave to intersect the surface of the water at an angle less grazing than the critical angle, which is about 13°, penetration effects similar to those described in this report should occur. But if the sub-Mach 4.5 aircraft should dive at such an angle (about 40° at Mach 1.3, for example) that part of the Mach cone was incident upon the surface of the water at an angle of less than 13°, acoustic energy from this part of the Mach cone would be transmitted across the air-water interface and would continue to propagate through the water as a coherent wavefront. The transmitted noise would not die out rapidly with depth and frequency, as would penetrating noise. The effects of this underwater transmitted sonic boom noise on the ocean ecology would be much more severe.

6.6 EFFECTS OF SURFACE WAVES

Waves on the ocean surface should have no significant effect on penetration of sonic booms into the ocean, so long as the waves are not so steep as to make possible the transmission of sound into the water at angles less grazing than the critical angle on patches of the ocean

surface. However, there has been little work,[14] theoretical or experimental, in this area of investigation.

6.7 EFFECTS OF SURFACE SHIPS

In the early stages of the experiment described in this report, it was observed that a surface float such as an inner tube could cause appreciable transmission of sound into the water in an area where only total reflection and accompanying shallow penetration of sound into the water would have otherwise occurred.

On the basis of this experience in an acoustically scaled simulation, it is predicted that a ship on the ocean surface which is exposed to an atmospheric sonic boom will cause significantly more noise to go into the water in the region of the ship, than would have ordinarily penetrated into the water. The physical mechanism for this would be the acoustic excitation of the ship, which is a nearly closed air-filled cavity floating on the surface, followed by reradiation of a portion of the acoustic energy into the water. This reradiated noise would not be attenuated rapidly with depth and frequency, as would penetrating noise. Urick[15] and his coworkers at NOL have probably observed such a reradiation phenomenon in full-scale sonic boom experiments conducted at sea.

ACKNOWLEDGEMENTS

Mr. Charles Foster and Mr. Harry Close of DOT and Mr. Stan Oleson and Dr. John Powers of FAA contributed valuable suggestions and guidance during the conduct of this work. Mr. David Hilton of NASA/Langley was most helpful in providing the microphones used in the experiment. At Hydrospace, the overall effort was supervised by Mr. Damon Gray, who also contributed much valuable guidance. Finally, the successful wintertime conduct of the experiment was made possible largely by the willing efforts of Mr. David Smiley and Mr. Allan Bartles of Hydrospace.

REFERENCES

1. Young, R. W., "Penetration of Sonic Booms into the Ocean", paper presented at May 1968 meeting of the Acoustical Society of America (reprint of paper available from author; for abstract, see Journal of Acoustical Society of America 44, 392).

2. Brekhovskikh, Waves in Layered Media, Academic Press, New York (1960). p. 15-25.

3. Sawyers, "Calculated Underwater Pressure Levels from Sonic Booms", Stanford Research Institute Interim Technical Report 8 (December 1967).

4. Sawyers, "Underwater Sound Pressure from Sonic Booms", JASA 44, 523 (1968).

5. Cook, "Penetration of a Sonic Boom Into Water", paper presented at November 1967 ASA meeting and accepted for future publication in JASA (preprint of paper available from author; for abstract, see JASA 42, 1213).

6. Young, J. R., "Energy Spectral Density of the Sonic Boom", JASA 40, 496 (1966).

7. Bendat and Piersol, Measurement and Analysis of Random Data, John Wiley & Sons, New York (1968), p. 82.

8. Wenz, "Acoustic Ambient Noise in the Ocean: Spectra and Sources", JASA 34, 1936 (1962).

9. Hilton and Newman, "Instrumentation Techniques for Measurement of Sonic Boom Signatures", JASA 39, S31 (1966).

10. Waters, "Calibration of Hydrophones Used in Sonic Boom Simulation Experiment", HRC TN 122, May 1970.

11. Hudimac, "Ray Theory for the Sound Intensity in Water Due to a Point Source Above It", JASA 29, 916 (1957).

12. Horton, C W , Fundamentals of Sonar, U. S. Naval Institute (1957), p. 119.

13. Urick, Principles of Underwater Sound for Engineers, McGraw-Hill, Inc. (1967), p. 166.

REFERENCES (Contd.)

14. Macaluso, "On the Transmission of Sound from a Monopole Source Through a Finite, Corrugated Boundary between Fluid Media", Ordnance Research Laboratory TM 214-02 (February 1970).

15. Urick, Lund and Colvin, "An Underwater Observation of a Sonic Boom", NOLTN 7946 (March 1968); Colvin; "Underwater Characteristics of a Sonic Boom", NOLTN 8034 (June 1968). These are U. S. Naval Ordnance Laboratory Internal Memos, which are not for external distribution. They are the sole responsibility of the authors.